Gasification: Part I. Isothermal, Kinetic Control Model for a Solid with a Pore Size Distribution

A model describing the development of specific surface area, volume, porosity, and mean pore radius of a porous solid with extent of gasification is developed based on consideration of pore size growth, initiation of new pores, and coalescence of adjacent pores. Use of population balances and formulation of the properties as moments of the pore size distribution leads to a mathematically simple, closed set of equations for kinetically controlled gasification. The model successfully predicts maximums in specific surface area and number of pores observed by Kawahata and Walker (1962) in the activation of devolatilized anthracite by CO_2 in a fluidized bed.

KENJI HASHIMOTO
and
P. L. SILVESTON

University of Waterloo
Waterloo, Ontario, Canada

SCOPE

This paper is a contribution to the modeling of heterogeneous reactions between parts or all of a porous solid phase and gaseous components, usually oxidants. Heterogeneous systems of this type are encountered in partial gasification to form activated carbon, burning of porous solid fuels, regeneration of coked catalyst, roasting of ores, and certain types of metathesis reactions where gaseous products are formed. Although the model developed in this paper and its formulation are generally applicable to heterogeneous reactions, they should be particularly valuable where the physical properties of the solid phase, such as surface area or mean pore size, are important. One such case is partial gasification of chars to form activated carbon. Indeed, the objective of the study discussed in this paper was to predict the degree of gasification required to maximize either the surface area or the number of pores in a solid (Hashimoto and Silveston, 1972).

The chemical engineering literature is quite rich in models for heterogeneous reactions. These can be grouped as homogeneous or as shrinking core models. The former were developed independently by Walker et al. (1959) for gasification and by Ausman and Watson (1962) for catalyst regeneration and Lacey et al. (1965) for absorption of SO_2 by MnO_2. In these models and their more recent extensions (Ishida and Wen, 1968; Kito et al., 1969; Wen, 1968), the heterogeneous reaction proceeds throughout the solid, but at rates depending upon the radial position of the point and the effective diffusivity. In the shrinking core models the diffusional resistance within the solids is assumed to be so large that the reaction is confined to a plane, or if there is no solid product, to the external surface of the solid. The original model of Yagi and Kunii (1955) has been extended to nonisothermal systems by Hills (1967, 1968), Shen and Smith (1965, 1966), and Wen and Wei (1971). Ishida and Wen (1968) have constructed a general model which includes the homogeneous and shrinking core models as special cases.

Both sets of models have been applied successfully to a variety of reaction systems (see Anastasia et al., 1971; Costa and Smith, 1971; Hills, 1967; Hills, 1968; Mendoza et al., 1970; Rigg, 1970; Scrivner and Manning, 1970). They suffice if the density or conversion of the solid phase is to be found as a function of time. All these models are macroscopic and incapable of describing changes in pore size or surface area through reaction except with the aid of auxiliary empirical expressions. Wen (1968), for example, uses an empirical relation to relate effective diffusivity to conversion. An extension of current theory, then, is required if a description of pore properties is desired. Applications in which this additional insight would be useful are activation of carbon, matrix acidification of oil bearing rock (Guin et al., 1971; Schechter and Gidley, 1969), or in reactions where large changes in intraparticle effective diffusivity are encountered.

Microscopic consideration of pore size change has been undertaken by Petersen (1957) and Thomas (1966). A model for time rate of change of the average radius of a cylindrical pore was obtained by Petersen and extended to a network of intersecting pores. Thomas dealt with a single conically shaped pore. Our contribution has been to take the microscopic approach and construct a macroscopic model which predicts measurable properties of the solid such as surface area porosity, mean pore radius, particle radius as a function of either time or extent of reaction. Allowance for pore size distribution in the solid has been made through the use of population balances in the derivation. Schechter and Gidley (1969) tackled the problem of matrix acidization of porous oil bearing rock in a closely related but independent paper using the approach of our paper. Experimental confirmation of the model they obtained was recently published (Guin et al., 1971).

CONCLUSIONS AND SIGNIFICANCE

The population balance technique (Himmelblau and Bischoff, 1968; Hulbert and Katz, 1964) originally applied to particulate solids (Hulbert and Akiyama, 1969; Hulbert and Stefango, 1968; Tsuchiya et al., 1966) has been extended to systems of pores to provide a detailed model describing gas-solid reactions in porous solids.

Reaction is considered on a microscopic scale by allowing for pore growth, initiation of new pores, and coales-

Correspondence concerning this paper should be addressed to P. L. Silveston. K. Hashimoto is with Kyoto University, Kyoto, Japan.

cence of adjoining pores. Each of these phenomena contribute to change the number of pores of radius r per unit volume of the solid and thereby the pore size density distribution function at some specific point within the solid. The symbolic statement of the rate of change in the distribution function is given by Equation (1). The purely mathematical operations of multiplying this equation by r^n and integrating over the possible range of pore size generates a set of n differential equations in terms of the moments of the density distribution function, illustrated by Equation (2). Properties of the solid such as specific surface area or most probable pore radius can be expressed in terms of moments through the relations given in Table 1. Integration of the moment equations, therefore, provides a prediction of the change of solid properties with time.

A model for a specific gas-solid reaction is obtained by introducing expressions for pore growth, initiation, and coalescence, as well as auxiliary expressions for rate of reaction, particle shrinkage, and mass transport to and within the solid. Equations (28) to (32) in this paper were derived for a gasification reaction in which most of the solid mass may be consumed, the particle shrinks and diffusional resistances without and within the solid are negligible. The reaction was assumed to be first order in the gaseous oxidant. Equations (34) to (37) restate the gasification model in terms of the extent of gasification. Gasification was chosen for modeling because of the lack of detail provided by models currently available for this process.

Partial gasification data of Kawahata and Walker (1962) obtained on devolatilized anthracite were used to test the model. Figures 1a and 1b show that the model accurately predicts maximums in the relative specific surface area and relative specific total number of micropores with burn off observed experimentally. The agreement is surprisingly good considering that two of the ten parameters appearing in the model [Equations (34) to (37)] are calculated from devolatized anthracite properties alone, while four more were evaluated from data at low burn-off well away from the region of the maximum.

Conclusions to be drawn from this work are that the population balance approach is applicable to gas-solid reactions, that the approach provides a detailed model of this class of reactions, and that assumptions employed for the pore growth, initiation, and coalescence and for the kinetics of this gas-solid reaction, etc., lead to a satisfactory model for the gasification of a solid. Schechter and Gidley's contribution (1969) confirm the first conclusion.

The primary significance of this work is that it makes available a detailed solid gasification model which should be useful for designing gasification systems or for interpreting experimental observations. Allowance was made for size distributions, in this case of cavities within the solid known to exist, but neglected in all current gas-solid models. In the following, this contribution shows the steps to be taken and indicates where assumptions and simplifications must be made to derive gas-solid reaction models using the population balance approach.

MODEL DEVELOPMENT

If the distribution of pore sizes can be stated in terms of a characteristic radius r of a pore, the change in the distribution with time due to a gas-solid reaction is given by

$$\frac{\partial f}{\partial t} + \frac{\partial}{\partial r}\left(f\frac{dr}{dt}\right) - B + D = 0 \qquad (1)$$

This is derived from a general expression proposed by Hulburt and Katz (1964) and later restated by Himmelblau and Bischoff (1968) who used the term population balance for the equation. Although introduced for particles or distinguishable elements of a fluid, the general expression should apply equally well to void space such as a pore within a solid. Indeed, we derive Equation (1) from first principles elsewhere.* In Equation (1), f is a density distribution function, that is, fdr is the number of pores having a radius lying between $r - dr/2$ and $r + dr/2$ at time t in an appropriate unit volume at some arbitrary point in the solid. The term B is the rate of introduction of new pores of the radius range into the unit volume at time t, while D is the rate of removal of pores (through coalescence). B and D are referred to as the birth and death terms respectively.

Hulburt and Katz point out that Equation (1) may be transformed into moment equations which are often easier to solve and frequently provide a more convenient description of the physical system. Multiplying Equation (1) by r^n and integrating from 0 to ∞ yields

$$\frac{\partial M_n}{\partial t} - n\left\langle r^{n-1}\frac{dr}{dt}\right\rangle + \int_0^\infty r^n (D - B)\,dr = 0 \qquad (2)$$

for the nth moment, M_n, where

$$\left\langle r^{n-1}\frac{dr}{dt}\right\rangle = \int_0^\infty r^{n-1}\left(\frac{dr}{dt}\right) f\, dr$$

and n is limited to zero and positive integers.

With the exception of the most probable pore radius, defined and related to the moments as

$$\bar{r} = \frac{\int_0^\infty r\, f\, dr}{\int_0^\infty f\, dr} = \frac{M_1}{M_0} \qquad (3)$$

a pore shape must be assumed to express solid properties in terms of moments of the pore size distribution. The shape used will depend upon the particular gas-solid system under consideration. For the purposes of this paper, we assume a cylindrical pore. Since the model we eventually derive contains many adjustable parameters, errors due to a moderately inaccurate pore shape probably can be absorbed. The cylindrical pore assumption gives simple relations, and we recommend its use in the absence of pore shape information.

As a result of the shape assumption,

$$r_e = \frac{2\,V_m}{S_m} \qquad (4)$$

where V_m and S_m are the local specific pore volumes and surface areas. Assuming uniform pore length $\bar{l}$

$$S_m = \frac{2\pi\bar{l}}{\rho_B}\int_0^\infty r\, f\, dr \qquad (5)$$

The integral is the local first moment. Rearranging,

* A detailed manuscript is available from the authors.

$$M_1 = \frac{\rho_B S_m}{2\pi\bar{l}} \tag{6}$$

Table 1 summarizes the relations between moments and solid properties. The constant pore length assumption means that the total number of pores per unit weight, $N_m = L_m/\bar{l}$. Consequently, relative total pore length Λ_m is also the relative total number of pores.

In order to further develop a model from Equation (2), the pore growth term containing dr/dt and the birth and death terms must be evaluated. To do this, a specific class of gas-solid reactions must be considered and our model is no longer general. The assumptions introduced so far were needed to relate properties to moments. They could be acceptable for various classes of gas-solid reactions such as roasting, catalyst regeneration, or even carbon deposition in the coking of a catalyst.

APPLICATION TO GASIFICATION

By gasification, we understand a reaction in which almost all of the solid is capable of reacting with the gas to form only gaseous products. The inert solid phase is noncontiguous so the particle shrinks and on a micro scale walls separating pores can be eaten away, causing pores to coalesce. Familiar examples of gasification are combustion of solid fuels and activation of carbons with steam or carbon dioxide.

Since we have assumed the solid to be largely reactive, it is convenient to use an inert matter free basis. Thus, we consider the unit volume for our population balance to be of inert free solid and ρ_B is the apparent density of inert free solid.

Gasification, locally, may either expand the pore or initiate a new pore. Since the inert is incapable of forming an ash structure, the amount of reactive solid exposed per unit area is constant. Therefore the local gasification rate will depend on the gaseous reactant concentration, but not upon the local apparent density of the solid. For the purpose of this paper, gasification will be assumed to be first order in the oxidant.

A material balance on the solid in a slice normal to the pore axis gives for the local rate of pore growth

$$\frac{dr}{dt} = \frac{k_1 M_B c}{\rho_t} \tag{7}$$

where c is the oxidant concentration in a pore and M_B and ρ_t are the molecular weight and true reactive solid density respectively. Consideration of concentration gradients complicates the model. Therefore, in this paper we restrict ourselves to small particles and relatively low temperatures such that diffusional resistances can be neglected. Part II of this paper treats the diffusion problem. In the absence of concentration gradients, pore growth will be uniform. Equation (7) may be used for the change of the mean pore radius and bulk phase concentration C_g may be substituted for c.

The birth function B must recognize the possibilities of initiating new pores and forming a pore in the range $r \pm dr/2$ by the combination of smaller pores through gasification of the intervening wall. The initiation contribution to B, B_f, will be assumed to be kinetically similar to pore growth. Further, we assume that the micropores formed in this way have a single radius r_f. There is some justification for the radius assumption. Etch pits have been observed on carbon surfaces during gasification (Lamond and Marsh, 1964; Thomas, 1966) and associated with the crystallographic structure (Thomas, 1966). If we attribute pore initiation to an etching phenomena, then we would expect new micropores to exhibit dimensions conforming to the structure. The characteristic dimension or radius of the new pore, therefore, should be within a relatively narrow range. Consequently,

$$B_f = k_f C_g \rho_B \, \delta(r - r_r) \tag{8}$$

where k_f is a specific rate constant for pore initiation, δ is a Dirac delta function taking a nonzero value only when the pore radius is r_f.

The pore combination contribution B_c may be formulated assuming that only two pores coalesce. A critical problem is characterizing the pore formed. At the moment of coalescence, the volume of the new pore formed will be $\pi\bar{l}(r_1^2 + r_2^2)$ and the new surface $2\pi\bar{l}(r_1 + r_2)$ where r_1 and r_2 are the radii of the original pores. Making use of our radius convention,

$$r_c = \frac{r_1^2 + r_2^2}{r_1 + r_2} \tag{9}$$

where r_c is the characteristic radius of the new pore. Equation (9) may be linearized by noting that if $r_1 \approx r_2$, Equation (9) predicts $r_c \approx 0.5\,(r_1 + r_2)$, while if $r_1 >> r_2$, Equation (9) predicts $r_c \approx (r_1 + r_2)$. This suggests a linear form

$$r_c = \alpha(r_1 + r_2) \tag{10}$$

where $0.5 < \alpha < 1.0$.

Assuming that pores of any size r are randomly distributed, the joint probability that pores r_1 and r_2 are within the unit volume is $f(r_1)\,f(r_2)$. It is reasonable to assume that the rate of combination of r_1 and r_2 is proportional to the joint probability. Letting ϕ be the probability that adjacent pores grow sufficiently in the time period dt to come in contact, the rate of combination of r_1 and r_2 will be $\phi f(r_1) f(r_2)$ where the time and spatial coordinates are understood. Only combinations of r_1 and r_2 which yield a new pore of radius r interest us. These will be given by replacing r_2 by $(r/\alpha - r_1)$. The rate of formation of pores of size r at time t in the unit volume at a point in the solid will be the integral

$$B_c = \frac{1}{2}\phi \int_0^r f\left(\frac{r}{\alpha} - r_1\right) f(r_1)\, dr_1 \tag{11}$$

TABLE 1. MOMENTS AND LOCAL SOLID PROPERTIES

Property	Definition	Moment relation	Relative property
Specific pore length, L_m	$\frac{\bar{l}}{\rho_B}\int_0^\infty f dr$	$\frac{\bar{l}}{\rho_B} M_0$	$\Lambda_m = \mu_0/\rho_B{}^*$
Specific surface area, S_m	$\frac{2\pi\bar{l}}{\rho_B}\int_0^\infty r f dr$	$\frac{2\pi\bar{l}}{\rho_B} M_1$	$\Gamma_m = \mu_1/\rho_B{}^*$
Specific pore volume, V_m	$\frac{\pi\bar{l}}{\rho_B}\int_0^\infty r^2 f dr$	$\frac{\pi\bar{l}}{\rho_B} M_2$	$\Omega_m = \mu_2/\rho_B{}^*$
Most probable pore radius, $\bar{r}$	$\frac{\int_0^\infty r f dr}{\int_0^\infty f dr}$	M_1/M_0	$r^* = \mu_1/\mu_0$
Effective pore radius, r_e	$\frac{2V_m}{S_m}$	M_2/M_1	$\gamma_e = \mu_2/\mu_1$

Note: $\mu_n = M_n/M_n{}^0$ where $M_n{}^0$ is the initial value of the n^{th} moment and $\rho_B{}^* = \rho_B/\rho_B{}^0$ where $\rho_B{}^0$ is the initial apparent density.

where the 1/2 is necessary because the limits count the number of pores formed twice. Our random distribution assumption implies ϕ is independent of r.

The death term D, the removal of pores of radius r, will be the rate of combination of pores of radius r with pores of all other radii, or

$$D = \phi f(r) \int_0^\infty f(r_1)\, dr_1 \tag{12}$$

Substitution of Equations (7), (8), (11), and (12) into Equation (2) yields

$$\frac{\partial M_n}{\partial t} - \frac{n\, k_1\, C_g\, M_B}{\rho_t} M_{n-1} + \phi\, M_0\, M_n - k_f\, \rho_B\, C_g\, r_f^n - \frac{1}{2}\int_0^\infty \phi\, r^n \int_0^r f\left(\frac{r}{\alpha} - r_1\right) f(r_1)\, dr_1\, dr = 0 \tag{13}$$

The density distribution function f may be eliminated by introducing the approximation r/α for r in the upper limit of the inner integral in Equation (13). This change permits the double integral to be separated into the product of two integrals. The approximation for the last term in Equation (13) is then

$$B_c' = \frac{1}{2}\phi \int_0^\infty r^n \int_0^{\frac{r}{\alpha}} f\left(\frac{r}{\alpha} - r_1\right) f(r_1)\, dr_1\, dr \tag{14}$$

Changing the order of integration does not change the value of B_c' if the appropriate limits are used. Thus

$$B_c' = \frac{1}{2}\phi \int_0^\infty \int_{\alpha r_1}^\infty r^n f\left(\frac{r}{\alpha} - r_1\right) f(r_1) dr\, dr_1 \tag{15}$$

Letting $y = \frac{r}{\alpha} - r_1$, expanding the r^n term after substituting for r leads to a separable integral which may be written*

$$B_c' = \frac{1}{2}\alpha^{n+1}\phi \sum_{i=0}^{n} \binom{n}{i} M_{n-i}\, M_i \tag{16}$$

Replacing the last term in Equation (13) with Equation (16), and expanding gives

$$\frac{\partial M_0}{\partial t} - k_f\, \rho_B\, C_g + \phi \left(1 - \frac{\alpha}{2}\right) M_0^2 = 0 \tag{17}$$

$$\frac{\partial M_1}{\partial t} - \frac{k_1\, C_g\, M_B}{\rho_t} M_0 - k_f\, \rho_B\, C_g\, r_f + \phi\,(1 - \alpha^2)\, M_0 M_1 = 0 \tag{18}$$

$$\frac{\partial M_2}{\partial t} - \frac{2k_1\, C_g\, M_B}{\rho_t} M_1 - k_f\, \rho_B\, C_g\, r_f^2 + \phi\,(1 - \alpha^3)\, M_0 M_2 - \phi\, \alpha^3\, M_1^2 = 0 \tag{19}$$

The set of moment equations is closed. We have shown in the Table 1 that the M_0 to M_2 moments describe measurable solid properties so higher moments are not required.

To complete the gasification model, relations must be obtained for the apparent density which appears in Equations (17) to (19), porosity, conversion and particle shrinkage. The rate of change of apparent density (i.m.f.b.) and porosity are directly proportional to the gasification rate. Gasification, stoichiometrically, is

$$aA(g) + B(s) \rightarrow \text{Products}$$

where A is an oxidant and B the reactive solid. The rate of change in apparent density in terms of the local rate of gasification $\mathcal{R}_B$ is

$$\frac{\partial \rho_B}{\partial t} = -\mathcal{R}_B M_B \tag{20}$$

For a bidispersed pore size distribution, three processes contribute to gasification: enlargement of the micropores and macropores, and the formation of new micropores. The pore enlargement contribution is

$$\mathcal{R}_{Bm} = k_1\, C_g \int_0^\infty 2\pi\, r\, \bar{l} f(r) dr \tag{21}$$

Formation of new pores contributes

$$\mathcal{R}_{Bf} = \frac{k_f\, C_g\, \rho_B\, \rho_t\, v_f}{M_B} \tag{22}$$

where v_f is the volume of a newly open pore. To be consistent with our pore shape assumption, the new pore has a length $\bar{l}$ so that v_f can be expressed in terms of r_f. Diffusional resistances have been assumed to be negligible. Substituting, Equation (20) becomes

$$\frac{\partial \rho_B}{\partial t} + \left(2\pi\, k_1\, \bar{l} M_1 + k_f \frac{\rho_B\, \rho_t}{M_B} v_f\right) C_g\, M_B = 0 \tag{23}$$

Local gasification in terms of apparent density is

$$x = 1 - \rho_B/\rho_B^0 \tag{24}$$

Integrating over the solid, however, does not give the overall gasification because shrinkage of the solid particle also must be accounted for. Overall gasification (or burnoff) X must be found from an integral relation which for a spherical particle is

$$X = 1 - \frac{3}{(R_0)^3\, \rho_B^0} \int_0^{R_s} \rho_B\, R^2\, dR \tag{25}$$

where ρ_B^0, R_0 and R_s are the initial apparent density, initial particle radius, and momentary particle radius respectively.

Porosity is directly proportional to density and in terms of local conversion is

$$\theta = \theta^0 + \theta_B^0 x \tag{26}$$

where θ_B^0 is the initial volume fraction of the reactive solid and θ^0 is the initial porosity. Overall particle porosity does not depend on size change of the particle and so may be found by integrating local porosities.

Shrinkage arises from gasification of the external surface of the particle and abrasion of particles in equipment such as a fluidized bed. If we assume external gasification occurs by the same process as within the particle and further that the abrasion contribution is a constant fraction of gasification, rate of change of the particle radius will be

$$\frac{dR_s}{dt} = -\frac{k_1\, C_g\, M_B}{\rho_t}\left(\frac{1}{1 - \kappa}\right) \tag{27}$$

where κ is an abrasion factor.

In the gasification model, Equations (17) to (19) and (23) may be written as ordinary differential equations for the kinetically controlled gasification system assumed in this paper because local properties and thus moments will be the same throughout the particle at any time t. For integration purposes, initial values in terms of the initial

* Steps are given in a detailed manuscript available from the authors.

properties of the solid, $M_0^0 = \frac{\rho_B^0 L_m^0}{\bar{l}}$, $M_1^0 = \frac{\rho_B^0 S_m^0}{2\pi\bar{l}}$, $M_2^0 = \frac{\rho_B^0 V_m^0}{\pi\bar{l}}$ and ρ_B^0 and R_0 are necessary. The equations are nonlinear and highly coupled so analytical expressions for the properties as time functions are excluded.

Numerical integration may be simplified by making the dependent variables dimensionless using their initial values. The model becomes then

$$\frac{d\mu_0}{dt} - \frac{k_f \bar{l} C_g}{L_m^0}\rho_B^* + \frac{\phi_\infty \rho_B^0 L_m^0}{\bar{l}}\left(1 - \frac{\alpha}{2}\right)\phi^* \mu_0^2 = 0 \quad (28)$$

$$\frac{d\mu_1}{dt} - \frac{2\pi k_1 M_B C_g}{\rho_t}\frac{L_m^0}{S_m^0}\mu_0 - \frac{2\pi k_f C_g r_f \bar{l}}{S_m^0}\rho_B^* + \frac{\phi_\infty \rho_B^0 L_m^0 (1-\alpha^2)}{\bar{l}}\phi^* \mu_0\mu_1 = 0 \quad (29)$$

$$\frac{d\mu_2}{dt} - \frac{k_1 M_B C_g}{\rho_t}\frac{S_m^0}{V_m^0}\mu_1 - \frac{\pi k_f C_g r_f^2 \bar{l}}{V_m^0}\rho_B^* + \frac{\phi_\infty \rho_B^0 L_m^0 (1-\alpha^3)}{\bar{l}}\phi^* \mu_0\mu_2 - \frac{\phi_\infty \rho_B^0 \alpha^3}{4\pi\bar{l}}\frac{S_m^{0^2}}{V_m^0}\phi^* \mu_1^2 = 0 \quad (30)$$

$$\frac{d\rho_B^*}{dt} + k_1 C_g M_B S_m^0 (\mu_1 + \sigma \rho_B^*) = 0 \quad (31)$$

$$\frac{d\xi_s}{dt} + \frac{k_1 C_g M_B}{R_0 \rho_t}\left(\frac{1}{1-\kappa}\right) = 0 \quad (32)$$

In Equations (28) to (30), ϕ has been replaced by $\phi_\infty \phi^*$ where ϕ^*, the normalized combination function, is assumed to be a function of local extent of gasification and ϕ_∞ is the asymptotic value of ϕ at total gasification. The reason for this is that ϕ is time dependent. As pore initiation and growth proceeds, pores draw closer together and ϕ must increase. In Equation (31)

$$\sigma = \frac{k_f \rho_t}{k_1 M_B}\frac{\pi r_f^2 \bar{l}}{S_i^0}$$

Normalizing Equation (25),

$$X = 1 - 3\int_0^{\xi_s} \rho_B^* \xi^2 d\xi \quad (33)$$

where ξ is the radius of any position in the spherical particle at t relative to the original radius of the particle.

Change of particle radius with time suggests a moving boundary problem. However, if gasification is kinetically controlled, oxidant concentration is uniform throughout the particle and local properties, such as surface area, are independent of spatial position. Equations (28) to (31) are not coupled to Equation (32) so that the moving boundary problem does not arise.

In some gasification systems, such as the activation of char or coal, the variation of solid properties with extent of gasification is important rather than with time. Our model can be expressed in terms of extent of gasification by substituting Equation (24) in Equation (31) to obtain an expression for dx/dt. This expression may be used to eliminate time from Equations (28) to (30) and (32). Making use of the relations given in the last column of Table 1, the normalized moments may be replaced by the relative properties to give

$$\frac{d\Lambda_m}{dx} - \frac{\Lambda_m}{1-x} - \left[\frac{b_1}{(1-x)\Gamma_m} - \left(1 - \frac{\alpha}{2}\right) b_7 \frac{\Lambda_m^2}{\Gamma_m}\right]\left[1 + \frac{\sigma}{\Gamma_m}\right]^{-1} = 0 \quad (34)$$

$$\frac{d\Gamma_m}{dx} - \frac{\Gamma_m}{1-x} - \left[\frac{b_2 \Lambda_m}{(1-x)\Gamma_m} + \frac{b_3}{\Gamma_m(1-x)} - (1-\alpha^2) b_7 \Lambda_m\right]\left[1 + \frac{\sigma}{\Gamma_m}\right]^{-1} = 0 \quad (35)$$

$$\frac{d\Omega_m}{dx} - \frac{\Omega_m}{1-x} - \left[\frac{b_4}{1-x} + \frac{b_5}{(1-x)\Gamma_m} + \alpha^3 b_8 \Gamma_m - (1-\alpha^3) b_7 \frac{\Lambda_m \Omega_m}{\Gamma_m}\right]\left[1 + \frac{\sigma}{\Gamma_m}\right]^{-1} = 0 \quad (36)$$

$$\frac{d\xi_s}{dx} + \frac{b_6}{(1-x)\Gamma_m}\left(1 + \frac{\sigma}{\Gamma_m}\right)^{-1} = 0 \quad (37)$$

The coefficients appearing in the above equations are defined in Table 2. Not all are constants, b_7 and b_8 contain ϕ which we treat as a variable.

The model, Equations (34) to (37), has been written in terms of local properties. For kinetically controlled gasification, there are no local variations, so that the variables represent values for the entire particle. By the same token ρ_B^* in Equation (33) is independent of ξ and the equation can be integrated. Replacing the density by the local extent of gasification through Equation (24), overall conversion or burn-off in terms of local extent is

$$X = 1 - (1-x)\xi_s^3 \quad (38)$$

With this equation and numerically integrating Equations (34) to (37), property variations with conversion or burn-off may be calculated.

TEST OF THE GASIFICATION MODEL

Data reported by Kawahata and Walker (1962) were chosen to test our model. These researchers measured total micropore length, surface area, volume, and average pore radius as a function of burn-off for various narrow sieve fractions of devolatilized anthracite coal gasified by CO_2 in fluidized bed at 850° and 950°C. Macropore contributions were not given. They should be negligibly small compared to the micropore contributions. In such a case our model describes either total or micropore properties. To avoid confusion, we shall refer to micropore properties in the remainder of this paper and introduce the subscript

Table 2. Definition of the Coefficients in Equations (34) to (37)

$$b_1 = \frac{k_f \bar{l}}{k_1 M_B L_m^0 S_m^0} \qquad b_5 = \frac{\pi k_f r_f^2 \bar{l}}{k_1 M_B S_m^0 V_m^0}$$

$$b_2 = \frac{2\pi L_m^0}{\rho_t (S_m^0)^2} \qquad b_6 = \frac{1}{(1-\kappa)\rho_t R_0 S_m^0}$$

$$b_3 = \frac{2\pi k_f r_f \bar{l}}{k_1 M_B (S_m^0)^2} \qquad b_7 = \frac{\rho_B^0 L_m^0 \phi}{k_1 M_B C_g \bar{l} S_m^0}$$

$$b_4 = \frac{1}{\rho_t V_m^0} \qquad b_8 = \frac{\rho_B^0 S_m^0 \phi}{4\pi k_1 M_B C_g \bar{l} V_m^0}$$

i on a variable or parameter to indicate this reference. Kawahata and Walker's calculations indicated that for the 850°C data for 42 × 65 mesh devolatilized anthracite gasification was kinetically controlled.

Applicability of our model to Kawahata and Walker's results and, in particular, our demonstration that the system was kinetically controlled, are discussed elsewhere (Hashimoto and Silveston, 1972). Equations (34) to (38) and Table 2 give the form of the model appropriate to the experimental measurements.

Coefficients b_2 and b_4 could be obtained directly from Kawahata and Walker's data for the solid. The other coefficients contained rate constants, which could not be obtained from the literature, and the model parameters α, $\bar{l}$ and r_f, all arising from assumptions made in the model development. It was necessary, therefore, to evaluate the remaining coefficients α and σ from experimental data. Coefficients b_1, b_3, b_5 and σ were obtained from data at low burn-off where the combination rate function ϕ is negligibly small. Data at burn-off between 30 and 50% were used to calculate b_6, b_7, b_8 and α. Details of the calculations and the values obtained are given in another paper by the authors (1972) and in an unpublished manuscript.*

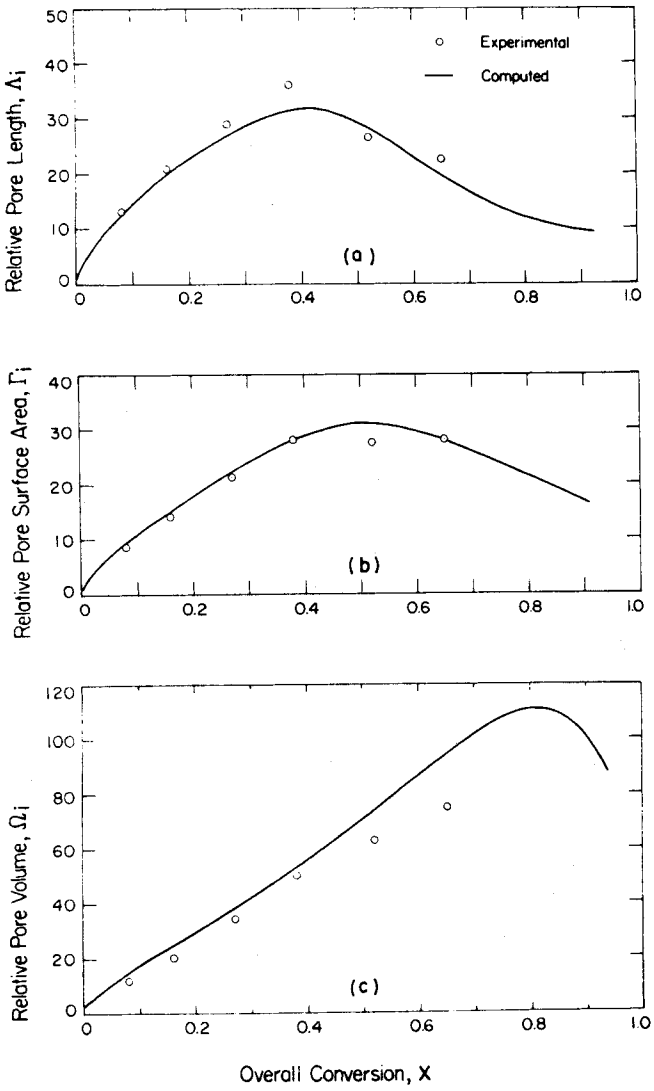

Fig. 1. Relative micropore pore length, surface area, and pore volume as functions of burn-off (experimental data for gasification of devolatilized anthracite coal from Kawahata and Walker).

* Manuscript available from the authors.

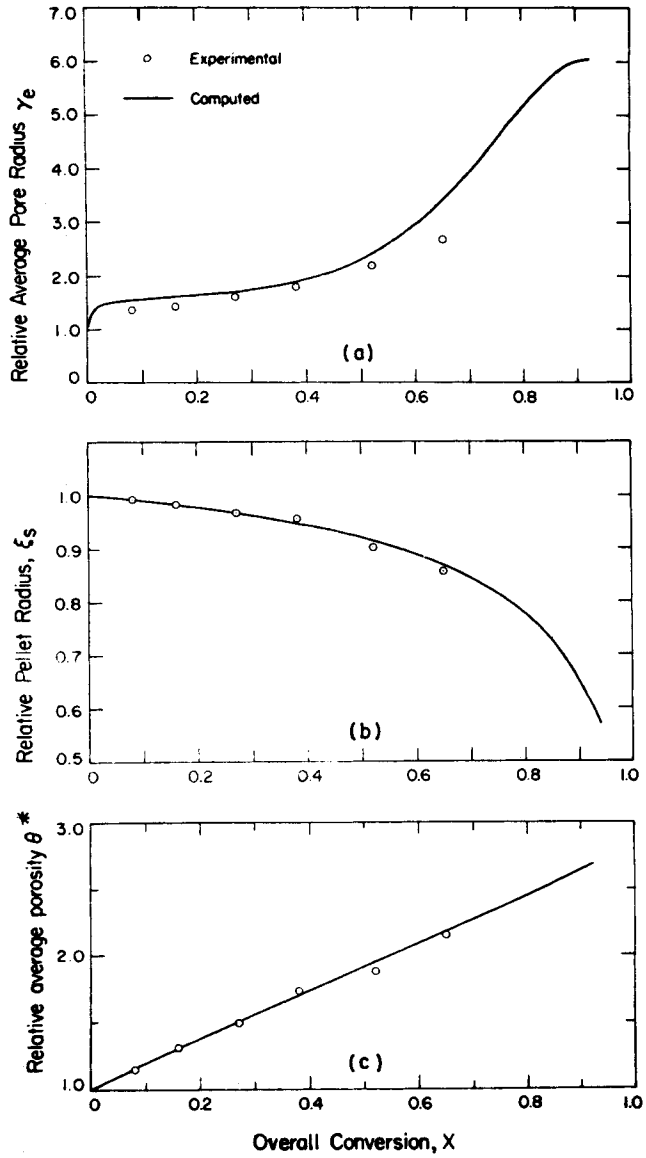

Fig. 2. Relative micropore pore radius, pellet radius, and average porosity as functions of burn-off (experimental data for gasification of devolatilized anthracite coal from Kawahata and Walker).

As expected, b_7 and b_8 were strong functions of extent of gasification with zero values at the start of gasification. The coefficient b_6 which appears in the shrinkage expression, Equation (37), was also found to depend on extent of gasification. The shape factor found $\alpha = 0.81$ lies about in the center of its possible range of 0.5 to 1.0. σ reflects the ratio of gasification by pore initiation to that by pore enlargement. The value of 3.5 indicates the importance of pore initiation for this system and confirms the suggestion made by Kawahata and Walker (1962) in their paper.

Integration of the model equations as described in Part II of this paper leads to plots of the relative properties of the devolatilized anthracite versus burn-off X shown in Figures 1 and 2.

Figures 1a and 1b show that the model predicts satisfactorily the experimentally observed maxima in the relative specific number of micropores (or micropore length) and relative specific micropore surface area. Figure 1b is particularly significant because the specific surface area is often closely related to the adsorption capacity of an active carbon. The capability of predicting the burn-off

needed to maximize surface area, which our model provides, should be useful in the manufacture of activated carbons by the partial gasification of chars.

Experimental data of Kawahata were limited to less than 65% gasification. In this range, the experimental relative specific micropore volume Ω_i has no maximum. However, our model in Figure 1c predicts a maxima at 80% burn-off. On physical grounds, a maximum is to be expected at high burn-off since rapidly dropping particle size, shown in Figure 2b after $X = 0.65$, counteracts pore combination and enlargement. Up to $X = 0.45$, our model fits the experimental values closely. Above this burn-off, the predicted Ω_1 deviates from experimental values. A better agreement for the higher range could be achieved by decreasing α. However, this change produced a poorer fit for Γ_1. The deviation observed for Ω_1 results from the linearized expression for r_c, Equation (10), the cylindrical pore assumption or perhaps from both these assumptions. A similar deviation is evident in the plot of the relative average pore radius γ_e in Figure 2a.

Figure 2a suggests the competing processes occurring in gasification. The relative average micropore radius changes only gradually from 5 to about 40% burn-off indicating that the micropore growth is balanced by the formation of new, fine micropores. Above 40% burn-off, pore numbers have decreased (Figure 1a) and sufficient pore growth has occurred to make pore combination an important process so that pore radius begins to increase sharply.

The relative pellet radius or shrinkage ratio ξ_s is plotted in Figure 2b. The excellent agreement between predicted and experimental shrinkage is due, no doubt, to using much of the shrinkage data to obtain b_6 in Equation (37). Figure 2c shows a nearly linear relation between burn-off and porosity as well as good agreement between the model and data. Linearity reflects the small contribution of shrinkage up to $X = 0.65$ and provides further support for a kinetically controlled rate in Kawahata's experiments. As shown in Part II, diffusion control increases the shrinkage contribution to X and causes relative porosity to increase less rapidly with burn-off.

Satisfactory representation of Kawahata and Walker's measurements suggests that the model we have obtained is adequate. Even though four of the ten coefficients were obtained using the important 30 to 50% burn-off range. It would seem fortuitous that proper choice of the coefficients alone produced the agreement. Examination of Equations (34) to (36) shows σ, α, and b_7 are common to all, so each of these equations has only one unique constant which was evaluated from the test data. It is unlikely that in this case the position of the maximum, curve shape, and the general model-data agreement can be attributed to just the choice of parameters.

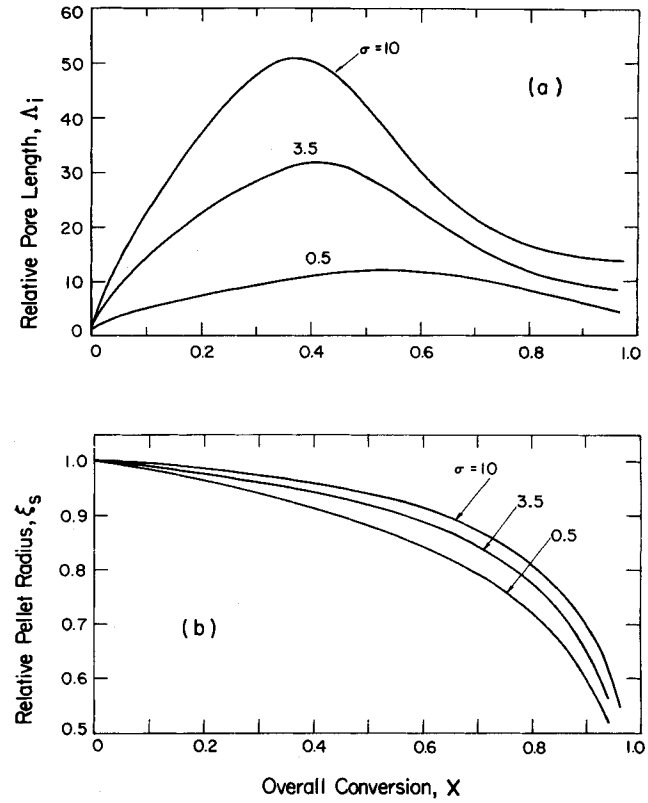

Fig. 3. Relative micropore pore length and number and relative particle shrinkage as functions of burn-off and the rate ratio σ.

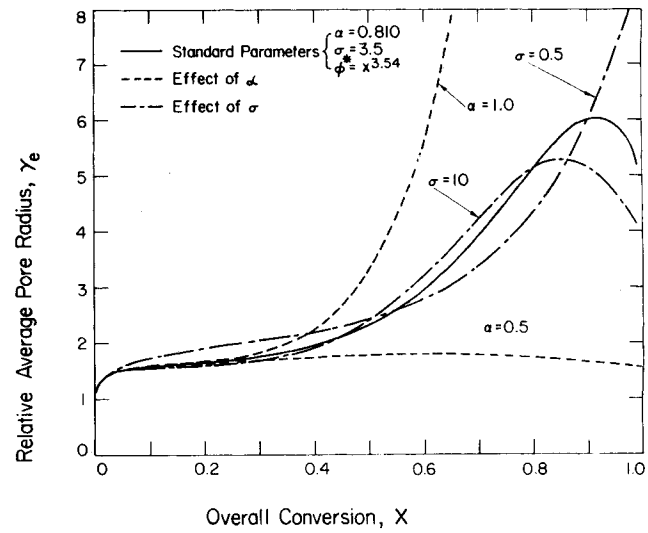

Fig. 4. Dependence of average relative pore radius on burn-off and the shape factor α and rate ratio σ.

INFLUENCE OF MODEL PARAMETERS

In the course of extracting model parameters from the Kawahata and Walker data it was found that the behavior of the model was particularly sensitive to the parameter σ, which is the ratio of the rate of gasification by pore initiation to the rate by pore growth, the pore radius combination coefficient α, and the functional form of the combination rate function ϕ. A direct measure of the effect of σ is Λ_i, the relative specific number of micropores. Figure 3a plots Λ_i versus X for $\sigma = 3.5$, obtained from the Kawahata and Walker data, and for two arbitrary values. Increasing σ increases Λ_i and the maximum appears at a lower burn-off because pore combination becomes important earlier. Gasification of the particle interior increases and particle shrinkage is less at the same level of burn-off. Figure 3b shows this effect. At any X, the shrinkage is least for $\sigma = 10$.

In Figure 4, the curves at high burn-off show that increasing σ decreases γ_e as expected since the greater pore initiation rate increases the number of fine pores. The inversion of the curves for $0.5 < X < 0.8$ arises because gasification of the particle interior is greater at higher σ for the same degree of burn-off. If γ_e were plotted against time rather than conversion, the $\sigma = 0.5$ curve would show the largest values of γ_e. Increased number of pores at any conversion contributes greater surface because the model assumes pores are established with length $\bar{l}$. Effect of σ on $\bar{\Gamma}_i$ is shown in Figure 5. For example, increasing

σ by 3-fold leads to a 50% increase in surface. The maximum Γ_i for $\sigma = 0.5$ is located at about $X = 0.7$ because shrinkage is favored over internal gasification at any X for this low value of σ. This behavior with σ suggest that finding means of increasing the initiation pore rate without accelerating pore growth would be an important improvement in processes for activating chars by partial gasification.

Figures 4 and 5 illustrate the effect of α on mean pore radius and surface area. The two extreme values of α and $\alpha = 0.81$ obtained from the devolatilized anthracite data are shown. The lower value, $\alpha = 0.5$ arises for the coalescence of equal sized pore, whereas $\alpha = 1$ for cases where one of the pores coalescing is much larger than the other. As Equation (11) is integrated over all pore sizes, letting $\alpha = 1$ inordinately increases γ_e and Γ_i since $r_c = \alpha(r_1 + r_2)$ and r_2 is not always less than r_1 as implied by this α value. On the other hand, $\alpha = 0.5$ severely underestimates pore growth due to combination. These two effects may be seen in Figure 4 and suggest the sensitivity of the mean radius prediction to α. The effect of α on γ_e is carried through to surface area as Figure 5 shows. Thus, the extreme value of α shows surface increasing unrealistically for all values of X. For $\alpha = 0.5$, Γ_i is lower, but a maximum does occur. Divergence of the α curves sets in beyond $X = 0.25$ suggesting that pore combination becomes important at this level of conversion for the devolatilized anthracite.

Estimates of b_7 and b_8 from Kawahata and Walker's data indicated that the ϕ is a strong function of burn-off or porosity. Figure 5 compares the development of surface area with conversion for the ϕ taken as a constant with that for the function $\phi^* = x^{3.54}$, obtained from the devolatilized anthracite data. The value of $\phi^* = 0.02$ chosen in Figure 5 corresponds to $X = 0.35$. No maximum occurs for this value, making it evident that a constant ϕ cannot predict the experimental surface area results. In the region where $x^{3.54} < 0.02$, the contribution of pore combination is exaggerated, whereas above $X = 0.75$, the contribution is greatly underestimated.

The sensitivity of the model to these parameters and the way in which they influence the behavior of the model seems to justify the modelling approach we have used.

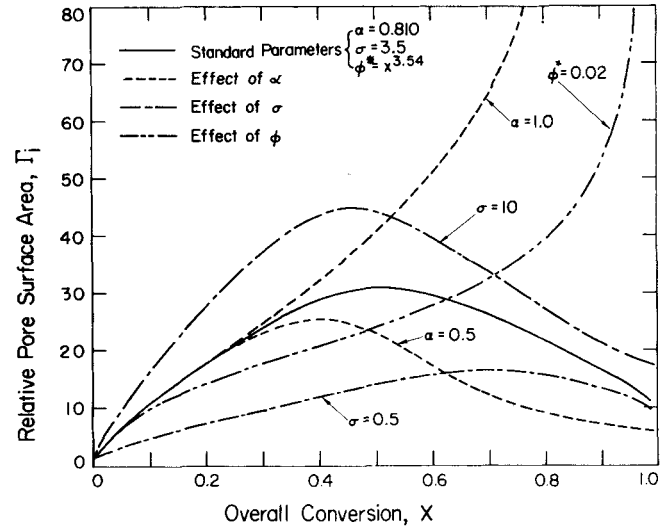

Fig. 5. Dependence of relative surface area on burn-off and the shape factor α, rate ratio σ, and the pore combination factor ϕ.

ASSUMPTIONS AND DIFFERENT USE OF THE POPULATION BALANCE

In the final section, we wish to examine the assumptions introduced to develop our gasification model. As pointed out earlier, the population balance approach does not seem to lend itself to the development of a general gas-solid reaction model so that for each class of reactions considered new sets of assumptions will be required.

The cylindrical pore and uniform pore length assumptions were necessary to relate properties to the moments of the pore size distribution. The cylindrical pore is a conventional assumption, but certainly other shapes are permissible with the restriction that surface and volume should be integer functions of powers of r to avoid noninteger moments in the model. Use of the cylindrical shape in our treatment leads to an adequate model. In view of the dearth of information on pore shape in solids, there seems to be no point in developing models for other pore shapes.

For rigor, pore length should be considered as a distributed variable. However, population balance theory has not been developed sufficiently at this point to undertake this extension. Assuming pore length to be proportional to radius, is an alternative to the single pore length assumption we have used. Surface area would be related then to the second moment, while pore volume would be obtained from the third moment. The expression, Equation (9), would change and higher moments would appear in the expression, Equation (23), for the rate of change of apparent density. The system of moments equations remain closed so the model could be integrated but instead of 3 moment equations, the model would consist of 4 moment equations. We have found no evidence for the alternative pore length assumption. Thus, we find no justification for the added moment equation this assumption introduces.

Schechter and Gidley (1969) avoid the shape problem in their study by choosing pore cross section as their distributed variable. This is permissible in their case because they are interested in permeability of the porous solid, and this property depends only upon cross section. However, if cross section is used as the distributed variable in our work, pore shape must still be assumed. With a cylindrical shape, specific surface area is related to the 1/2 moment of the distribution. We have not explored the use of noninteger moments in the model, but we anticipate that they would be inconvenient.

In deriving their expression for B_c, the pore combination contribution to the birth term, Schechter and Gidley consider the probability of another pore being present in the volume, $2\pi r\overline{l}\,dr$, a cylindrical pore grows during a time period dt. If the distributed variable is r rather than pore cross section, an r^{n+1} term is introduced into the integral of Equation (13) and a M_{n+1} moment appears in the third term of this equation. The system of moment equations generated, such as Equations (17) to (19) or (28) to (30), will not be closed. The system of equations cannot be integrated, or at best, higher order moments would have to be evaluated to see if their contribution is important. We avoid such a problem in our treatment by introducing a probability function to allow for pore combinations.

Other significant differences between our treatment and that of Schechter and Gidley are that their growth rate depends on pore cross section, whereas our rate is independent of pore dimension, and that they find the B_c term may be neglected, while this term is essential in our treatment.

Two approximations, one for r_c [Equation (10)] and the other a substitution of r/α for r, were introduced in

order to replace the integral in Equation (13) by an expression in terms of moments. Neither approximation has been investigated nor have we examined other methods of avoiding the problem the integral presents.

There is no restriction in the choice of rate expression except perhaps that rates dependent on pore shape may be limited to integer order of r and less than a square dependence to avoid noninteger moments and a nonclosed set of moment equations in the model. Allowing rate to depend on apparent density or use of a Langmuir-Hinshelwood kinetic model in place of the first-order model we employed does not introduce manipulative problems into the gasification model provided intraparticle diffusion may be neglected. First-order kinetics were used to follow convention in model derivation, but moreover because the oxidant order is frequently given as unity in models for carbon gasification. When diffusionally controlled gas-solid reactions are considered, as we do in Part II, non-first-order kinetics cause severe complications in an already mathematically difficult system because simple, or indeed even analytical, expressions for effectiveness factors are not obtained.

ACKNOWLEDGMENT

Support from a Water Resources Research grant of the Canadian Department of Energy, Mines and Resources, from the Faculty of Engineering, University of Waterloo, and the Japanese Ministry of Education is most gratefully acknowledged. Helpful discussions of our work were held with K. S. Chang (Waterloo), H. M. Hulburt (Northwestern), and P. L. Walker, Jr., (Penn. State).

NOTATION

A = oxidant
a = stoichiometric coefficient
B = rate of introduction of new pores of radius r, reactive solid
B_f, B_c = rate of introduction of new pores of radius r by pore initiation, by pore combination
b = coefficients in working equations of model (Table 2)
C_g = bulk concentration of oxidant
c = concentration of oxidant in a pore
D = rate of removal of pores of radius r
$f(r)$, f = pore size density distribution function
i.m.f.b. = inert matter free basis
k_1 = first-order specific rate constant for pore wall gasification
k_f = specific rate constant for pore initiation
L = specific total pore length
$\overline{l}$ = mean micropore length
M_B = molecular weight of carbon
M_n = nth moment about the origin
N = specific number of pores
n = moment index
R = radial position in the pellet
R_0 = particle radius at $t = 0$
R_s = particle radius at t
r = characteristic pore radius
r_e = effective preradius Equation (4)
r_c = radius of pore formed by coalescence
r_f = radius on pore formation
$\overline{r}$ = mean pore radius
R_B = local gasification rate
S = specific pore surface area
t = time
V = specific pore volume
v_f = pore volume on pore formation
X = overall gasification defined by Equation (25)
x = local gasification defined by Equation (24)
y = dummy variable

Greek Letters

α = pore radius combination coefficient defined by Equation (10)
Γ = relative specific pore surface area (Table 1)
γ_e = relative mean effective pore radius (Table 1)
δ = dirac delta or impulse function
θ = porosity, volume fraction
κ = abrasion factor
Λ = relative specific pore length or number (Table 1)
μ_n = nth relative or dimensionless moment = M_n/M_n^0
ξ = normalized radial position in particle = R/R_0
ρ_B^* = normalized apparent density = ρ_B/ρ_B^0
ρ_B = apparent density of the solid or of the reactive material (i.m.f.b.)
ρ_t = true density of the reactive solid
σ = rate ratio parameter
ϕ = combination rate function or combination probability function
ϕ^* = normalized combination rate function
ϕ_∞ = asymptotic combination rate function
Ω = relative specific pore volume (Table 1)

Subscripts

B = reactive solid phase
i = specific micropore property
m = specific total pore (micro plus macro) property
0 = state at $t = 0$, or zeroth moment
s = particle surface

Superscripts

$'$ = approximation
0 = state at $t = 0$
$*$ = normalized or relative variable

LITERATURE CITED

Anastasia, L. J., P. G. Alfredson, M. J. Steindler, "Reaction Model for the Fluorination of Uranium and Plutonium Compounds in Fluidized-Bed Reactors," *Ind. Eng. Chem. Process Design Develop.*, **10**, 150 (1971).

Ausman, J. M., and C. C. Watson, "Mass Transfer in a Catalyst Pellet During Regeneration," *Chem. Eng. Sci.*, **17**, 323 (1962).

Costa, E. C., and J. M. Smith, "Kinetics of Non Catalytic, Nonisothermal, Gas-Solid Reactions: Hydrofluorination of Uranium Dioxide," *AIChE J.*, **17**, 947 (1971).

Guin, J. A., R. S. Schechter, and I. H. Silberberg, "Chemically Induced Changes in Porous Media," *Ind. Eng. Chem. Fundamentals*, **10**, 50 (1971).

Hashimoto, Kenji, and P. L. Silveston, "Changes of Solid Carbon Properties During Gasification," paper presented at PACHEC Conf., Kyoto, Japan (1972).

———., "Gasification-Part II: Extension to Diffusion Control," *AIChE J.*, **19**, 000 (1973).

Hills, A. W. D., in *Hear and Mass Transfer in Process Metallurgy*, Inst. Mining and Metallurgy, U.K. (1967).

———., "The Mechanism of the Thermal Decomposition of Calcium Carbonate," *Chem. Eng. Sci.*, **23**, 297 (1968).

Himmelblau, D. M., and K. B. Bischoff, "Process Analysis and Stimulation," Ch. 6, Wiley, New York (1968).

Hulburt, H. M., and T. Akiyama, "Liouville Equations for Agglomeration and Dispersion Processes," *Ind. Eng. Chem. Fundamentals*, **8**, 319 (1969).

Hulburt, H. M., and S. Katz, "Some Problems in Particle Technology," *Chem. Eng. Sci.*, **19**, 555 (1964).

Hulburt, H. M., and D. G. Stefango, "Design Models for Continuous Crystallizers with Double Draw Off," *Chem. Eng. Progr. Symp. Ser.*, No. 95, **95**, 50 (1968).

Ishida, M., and C. Y. Wen, "Comparison of Kinetic and Dif-

fusional Models for Solid-Gas Reactions," *AIChE J.*, **14**, 311 (1968).
Kawahata, M., and P. L. Walker, Jr., "Mode of Porosity Development in Activated Anthracite," in *Proc. 5th Carbon Conf.*, **2**, 251-263, Pergamon, London (1962).
Kito, M., T. Onodera, and S. Sugiyama, *Kaguku Koguku* (Chem. Eng. Japan), **32**, 695 (1968); *Intern. Chem. Eng.*, **9**, 181 (1969).
Lacey, D. T., J. H. Bowen, K. S. Basden, "Theory of Noncatalytic Gas-Solid Reactions," *Ind. Eng. Chem. Fundamentals*, **4**, 275 (1965).
Lamond, T. G., and H. Marsh, "The Surface Properties of Carbon, III—The Process of Activation of Carbon," *Carbon*, **1**, 293 (1964).
Mendoza E., R. E. Cunningham, and J. J. Ronco, "Oxidation of Zinc Sulfide Pellets," *J. Catalysis*, **17**, 1, 194, 277 (1970).
Petersen, E. E., "Reaction of Porous Solids," *AIChE J.*, **3**, 443 (1957).
Rigg, T., "Hydrogen Reduction of the Chlorides of Bi-valent Chromium and Iron," *Can. J. Chem. Eng.*, **48**, 84 (1970).
Schechter, R. S., and J. L. Gidley, "The Change in Pore Size Distribution from Surface Reactions in Porous Media," *AIChE J.*, **15**, 339 (1969).
Scrivner, N. C., and F. S. Manning, "Reduction Kinetics of Swelling Wustite Particles," *ibid.*, **16**, 326 (1970).
Shen, J., and J. M. Smith, "Diffusional Effects in Gas-Solid Reactions," *Ind. Eng. Chem. Fundamentals*, **4**, 293 (1965).
Thomas, W. J., "The Effect of Oxidation on a Pore Structure of Some Graphitized Carbon Blacks," *Carbon*, **3**, 435 (1966).
Tsuchiya, H. M., A. G. Fredrickson, and R. Aris, "Dynamics of Microbial Cell Populations," in *Advances in Chem. Eng.*, **6**, 125, Academic Press, New York (1959).
Walker, P. L., Jr., Frank Rusinko, Jr., and L. G. Austin "Gas Reactions of Carbon" in *Advances in Catalysis*, **11**, 133, Academic Press, New York (1959).
Wen, C. Y., "Noncatalytic Heterogeneous Solid Fluid Reaction Models," *Ind. Eng. Chem.*, **160**, 34 (1968).
———., and L. Y. Wei, "Simultaneous Nonisothermal, Noncatalytic Solid-Gas Reactions," *AIChE J.*, **17**, 272 (1971).
Yagi, S., and D. Kunii in "5th Intern. Symp. on Combustion," 231, Reinhold, New York (1955).

Manuscript received April 2, 1971; revision received August 29, 1972; paper accepted October 13, 1972.

Gasification: Part II. Extension to Diffusion Control

Gasification model developed in Part I is extended to allow for mass transfer of oxidant to the particle and for intraparticle diffusion. For this extension, a moving boundary problem results which is solved numerically in conjunction with a two-point boundary value problem for the oxidant concentration profile in the particle. The extended model predicts, as expected, that mass transfer stifles gasification and intraparticle diffusion shifts gasification to the outer surface of the particle. For the conditions and parameters used in Part I, particle Thiele moduli above 10 result in particle shrinkage with negligible change in the solid properties, whereas if this modulus is less than 0.1, gasification is kinetically controlled.

KENJI HASHIMOTO and P. L. SILVESTON

University of Waterloo Waterloo, Ontario, Canada

SCOPE

In this portion we extend the gas-solid reaction model developed in Part I of this paper to cases where intraparticle diffusion must be considered. Our objectives in this extension are to further generalize the model, provide criteria which could be used to determine whether gasification is diffusionally or kinetically controlled, and finally to examine how mass transfer influences the development of solid properties with gasification.

Our model extension is applicable to systems where the physical properties of the solid undergoing gasification are important. An example is the partial gasification of chars to form activated carbon.

It is generally recognized that mass transfer is important in gas-solid reactions and it is taken into account in the shrinking core and homogeneous reaction models referred to in Part I. The approach followed in this paper to derive our model is similar to that used in the past as typified by Wen and co-workers (1963, 1968). Unlike Wen and others, a specific pore structure is considered. We assume a bidispersed pore size distribution in which the micropores account predominantly for surface area, porosity, and pore volume. The macropores serve as conduits carrying the oxidant and removing the gaseous products of the reaction. Our other assumptions are taken from Part I, for example, no ash remains after gasification so pore coalescence may occur and the particle size may change, micropores are uniform in length and cylindrical, and the gasification reaction is first-order in the oxidant.

Although we allow for enlargement of both micropore and macropores, micropores cannot become macropores and new pore initiation is limited to micropores.

Micropore shape is assumed not to change during gasification. The micropore size, therefore, is described by a mean pore radius and its change is related to gasification by measuring gasification as the flux of oxidant through the micropore mouth. This follows an approach suggested by Thomas (1966). Intraparticle diffusion of oxidant is handled through Fick's law using a variable effective diffusivity. Both Walker et al. (1959) and Wen (1963) before us have allowed the diffusivity to change during the reaction. Mass transfer to the particle is introduced conventionally as a boundary condition for the equation describ-